Modelling the effect of hydraulic conductivity variability on slope stability calculations for a site in South-East Quito, Ecuador

C. Zapata[1,2], E.A. Holcombe[1], P.J. Vardanega[1], E. Jiménez[3]

[1] University of Bristol, Bristol, UK
[2] College of Social Sciences and Humanities, Universidad San Francisco de Quito, Ecuador
[3] Facultad de Ingeniería en Geología y Petróleo, Escuela Politécnica Nacional, Ecuador

Abstract. Rainfall-triggered landslides are increasingly a concern in rapidly urbanising areas around the globe. Assessing the stability of slopes is important for geotechnical engineers and planners working in these regions. Saturated hydraulic conductivity is key parameter for assessing the hydrological drivers of slope instability. This paper presents a recent citizen-science case study in Quito, Ecuador, in which saturated hydraulic conductivity measurements were taken in the field on a fine-grained volcanic sediment, often referred to as cangahua, were obtained as part of the Tomorrow's Cities project on urban multi-hazards and disaster risk management. These data are then used along with a recent soil database of Quito soils (Quito/GEO-299) and other locally obtained soil data and the Combined Hydrology And Stability Model (CHASM) to assess the stability of slopes in a hillside community in South Quito. The paper focuses on the variability of key slope stability parameters, including saturated hydraulic conductivity to assess the plausible ranges of behaviour for slopes in this area.

Keywords: Slope stability, Cangahua, Hydraulic Conductivity, Urbanisation, Quito

1 INTRODUCTION

1.1 Assessing rainfall-triggered landslides in cities: a challenge for geotechnical engineers

Landslides triggered by rainfall cause significant economic loss, deaths, and injuries each year worldwide. More landslides are expected as climate change increases the frequency of extreme rainfall events (Picarelli *et al.* 2020) and of multi-annual climate variations such as El Niño Southern Oscillation (ENSO), which particularly affects rainfall patterns and associated landslide fatalities in the tropics (Emberson *et al.* 2021). Such disasters disproportionately affect the most socio-economically vulnerable communities and regions. Nearly one billion people in developing countries are vulnerable to disasters due to the physical conditions of their homes, high degree of exposure to hazards, and inadequate emergency systems (UN Populations Division 2018); and a quarter of the global population lives in poverty in informal settlements (UNDRR 2022). In the case of landslides, urban expansion onto the peripheral slopes of cities around the world is exposing a growing number of people to such hazards. Furthermore, the susceptibility of these slopes to landslides may be increased through unplanned and informal urbanisation actions such as deforestation, slope cutting, structural loading, and unmanaged drainage (e.g. Ozturk *et al.* 2022).

The scale and impact of rainfall-triggered urban landslides is exemplified in Quito, Ecuador, which has seen recurrent landslide disasters throughout its history as the city has grown (Watson *et al.* 2022). For example, the La Gasca disaster on 31st January 2022 occurred when heavy rainfall triggered multiple landslides in a ravine on the flanks of the Pichincha volcano above the city. The debris then combined with floodwater in the ravine and became a fast-moving mudflow that flooded through the La Gasca district on the lower slopes, leaving 28 dead and costing thousands of dollars in emergency response and reconstruction (Municipio de Quito 2022).

Geotechnical engineers and municipal authorities in Quito and similar landslide-prone cities face the task of addressing existing landslide risks, applying appropriate geotechnical design standards on slopes, and identifying resilient urban development strategies for the future. Slope stability and landslide hazard assessments provide the basis for such practices and policies. If the effects of current and future land use and rainfall scenarios are to be accounted for then physics-based models are needed – for example, using limit equilibrium analysis methods or finite element analysis. Including dynamic hydrology in slope stability models allows rainfall-triggered landslide hazards to be estimated with respect to rainfall events of a specific intensity and duration (Almeida *et al.* 2017). Such models represent rainfall infiltration, unsaturated and saturated seepage, and changes pore water pressures over time. They typically require input data such as the saturated hydraulic conductivity (k_{sat}), soil moisture characteristic curves, and the initial soil moisture content of soils. Furthermore, to assess the effect of urbanisation on slopes it is important to represent the features of the built environment, such as unsupported cut slopes, that may increase landslide hazard locally (Holcombe *et al.* 2016). This approach to slope stability assessment therefore requires high resolution topographic data and information on soil hydrological properties that is not usually collected as part of a standard geotechnical investigation for slopes. Obtaining the necessary data is the first challenge that geotechnical engineers must tackle to assess and address current and future urban landslide hazards.

1.2 Geotechnical data for modelling slope hydrology and stability: Quito's cangahua soils

Previous slope hydrology and stability modelling studies have shown that slope Factor of Safety (F), can be as sensitive to uncertainties in future rainfall intensities and durations under climate change as it is to uncertainties soil geotechnical properties (Almeida *et al.* 2017). Sensitivity analyses indicate the most influential geotechnical parameters are often the apparent effective cohesion, c' (which may be used in slope stability modelling to account for soil cementation, structure and root reinforcement – see Hubble *et al.* 2013 and Wu *et al.* 1979 for detailed analysis of the effect of vegetation on the c' parameter), angle of friction, and saturated hydraulic conductivity of the top stratum (Almeida *et al.* 2017, Bozzolan *et al.* 2020, Shepheard *et al.* 2018). Uncertainties in these parameter values arise from the natural heterogeneity of soils, biases in laboratory or field-testing procedures, human error, and sparse sampling at city scales – a particular challenge in resource-limited locations.

Geotechnical engineers in Quito also face the challenge of characterising the geotechnical properties of the volcanic sediment 'cangahua' soil found throughout the Ecuadorian and Colombian Andean Mountain range (O'Rourke and Crespo 1988). Cangahua is described by Vera and Lopez (1992) as a soft, porous rock (also found as an unconsolidated material, i.e., a soil) which is the product of the partial diagenesis of fine volcanic material (ash smaller than 2mm) cemented by amorphous clayey material, silica, iron oxides, or calcite. Crespo (1987) defined the granulometric properties of the cangahua, measured ranges of porosity of 56% to 43%, and noted that cangahua samples could not be fully saturated in the laboratory but reached maximum saturation ratios of about 90%. Crespo (1987) also noted that the strong cementation and coarse texture of the grains in cangahua presents several problems for characterizing the soil using standard geotechnical testing techniques.

Hen-Jones *et al.* (2022) and Othman *et al.* (2022) present statistical analyses of geotechnical parameter values for cangaua based on the comprehensive review and collation of publicly available reports and scientific papers. Othman *et al.* (2022) outlines the resultant development of a Geotechnical Database for Quito (Quito/GEO-299). However, there was extremely limited data on k_{sat} available in the public domain. To address this gap, the authors trialled the use of double-ring infiltrometry to measure cangahua k_{sat} in an informal hillside community (Zapata *et al.* 2023). The results were compared with values estimated using new empirical-statistical transformation equations (Feng 2022). Values of k_{sat} (m/s) of the same order of magnitude were obtained when Feng's (2022) equation for coarse soils was applied (Zapata *et al.* 2023).

1.3 Research questions

This paper presents an initial evaluation of the effect of variations in k_{sat} on the simulated stability of slopes in Quito. For a typical informal hillside community, the following questions are addressed:
1. How can key topographic and geotechnical properties be estimated for modelling these slopes?
2. How much influence do variations in k_{sat} have on the calculated stability of these slopes, and therefore, when is k_{sat} data needed for urban slope design and landslide hazard assessment?

2 EXPERIMENTAL DESIGN AND DATA

This study adopted a parametric modelling approach using the Combined Hydrology And Stability Model (CHASM) to represent the dynamic hydrology and properties of urban slopes prone to rainfall-triggered landslides. An urban hillside study site with a known cross-sectional geometry was selected, and 90 CHASM simulations were run to explore the effect on slope stability of a range of values of c', ϕ', k_{sat} and rainfall intensity. The model, dataset and experimental design are described below.

2.1 Modelling dynamic slope hydrology and stability response

CHASM is a physics-based model that represents rainfall infiltration, unsaturated and saturated groundwater seepage, changes in positive and negative pore water pressures, and slope F over time for two-dimensional slope cross-sections (Anderson and Howes 1985 and Wilkinson *et al.* 2002). It has been applied widely to assess slopes in the built environment, particularly in the humid tropics and in regions with deep soil profiles and has proven reliable for predicting the safe/failed condition of such slopes (e.g. Anderson 1990).

For the hydrological component of CHASM the slope cross-section is represented as a regular two-dimensional grid of cells, each with a soil type defined in terms of k_{sat}, soil water characteristic curves (SWCC), saturated moisture content, effective shear strength, dry and saturated unit weight. An initial water table and the slope surface matric suction are assigned. CHASM then uses a forward explicit finite-difference scheme to solve Richards' and Darcy's equations (Richards 1931, Darcy 1856) for unsaturated and saturated seepage each timestep (usually 10-60s). At the end of each simulation hour the pore water pressure field is incorporated into a limit equilibrium analysis. An automated search method is used to implement Bishop's circular method of slices (Bishop 1955) and the location of the slip circle with the minimum F is recorded for that hour. For simple design storm simulations, the first 7 days of simulation time have no rainfall to allow seepage to reach steady state, then a rainfall event is imposed followed by a second period with no rainfall to allow the groundwater conditions to respond. A comprehensive description of the model and equations used in CHASM is provided in Anderson and Howes (1985) and Wilkinson *et al.* (2002).

2.2 The case study dataset and simulation design

The site chosen for this study was San Luis de Miravalle community, located on landslide-prone unconsolidated colluvial cangahua slopes in south-east Quito. First, the following data was acquired:
*   10cm-resolution digital elevation model from a drone orthophoto survey indicating natural slope angles of 25 to 40° and cut slopes of 56 to 90° associated with houses and roads.
*   Daily rainfall volumes from a newly installed rain gauge monitored by community residents.
* k_{sat} measurements of 1×10^{-5} to 1×10^{-6} m/s obtained via double-ring infiltrometry and compared with values estimated from the soil particle size distribution (for details on the field testing and k_{sat} estimation see Zapata *et al.* 2023).

The location of the double-ring infiltrometer tests (Fig. 1a) was typical of slopes throughout the community in respect of the natural slope angle, cut slope geometry, soil profile, and land use. It was selected for this study and the cross-section was represented in CHASM as shown in Fig. 1b.
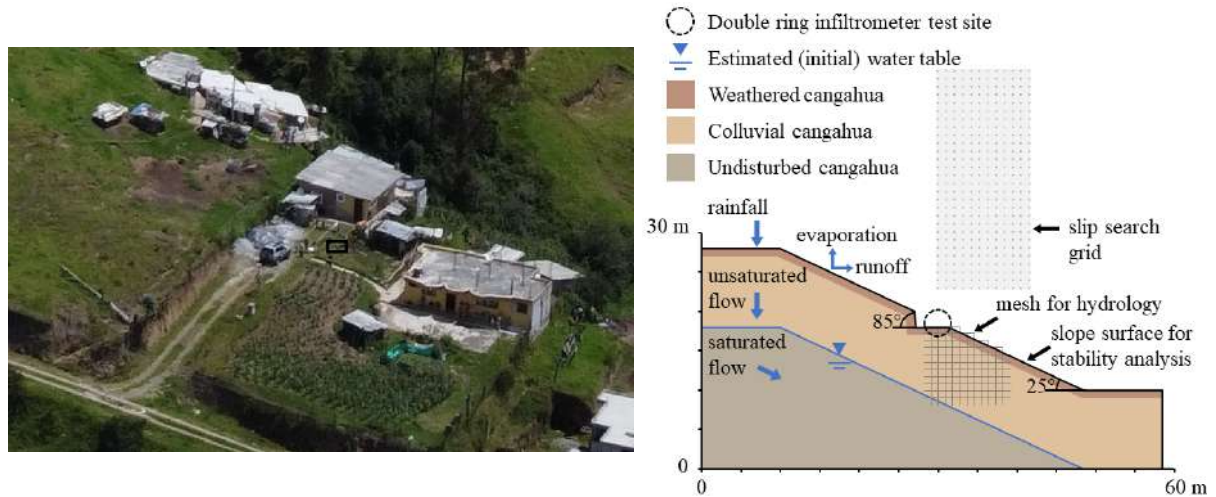
Figure 1. a) Aerial photo of study site indicating the location of double ring infiltrometer test for measurement of k_{sat} (photo credit: C. Zapata); b) Representation of study site cross section in CHASM

Table 1. Slope data and selected input parameter values for CHASM parametric simulations

CHASM input parameters*	Symbols (units)	Data source	Statistical Distribution **	Typical range	Values for simulations
Slope geometry:					
Natural slope angle	α (°)	Drone mapping	G (11.31, 2.19)	20-40	25
Cut slope angle	β (°)	"	W (3.42, 64.76)	56-90	85
Cut slope height	h (m)	"	G (5.54, 0.69)	0.5-6	2
House/ road width	w (m)	"	G (12.64, 0.51)	3-11	6.4
Thickness of colluvial cangahua stratum	T (m)	Geophysical & direct observations	-	5-20	10
Geotechnical properties of colluvial cangahua stratum:					
Apparent effective cohesion	c' (kPa)	Quito Geotechnical Database (Hen-Jones *et al.* 2022, Othman *et al.* 2022)	LN (3.8, 0.73)	5-100	5, 15, 30, 65
Effective friction angle	ϕ' (°)		N (33.43, 7.02)	20-55	24, 34, 44
Bulk unit weight	γ (kN/m³)		N (14.46, 1.82)	-	17.5
Saturated hydraulic conductivity	k_{sat} (m/s)	Double ring infiltrometer (Zapata *et al.* 2023)	-	1×10^{-5} - 1×10^{-10}	1×10^{-5}, 1×10^{-6}, 1×10^{-8} ***
Rainfall and initial groundwater conditions:					
Rainfall intensity	I (m/h)	Citizen science	-	-	5, 10 ****
Rainfall duration	D (h)	"	-	-	24
Initial water table depth	wt (m)	Direct observations	-	-	10

* Van Geunchten parameters for a Sandy Clay Loam were used for the SWCC: saturated and residual moisture contents = 0.413 and 0.149 m/m, α_{VG} = 0.644, n = 1.1535 (Hodnett and Tomasella 2002).
** Statistical distributions are: G = Gamma, LN = Lognormal, N = Normal, W = Weibull.
*** Values of $k_{sat} < 1\times10^{-8}$ m/s were not simulated for the colluvial cangahua stratum due to the imperceptible hydrological response over time for the simulated two-week timescales.
**** Rainfall intensities are based on 24-hour rainfall events that triggered landslides near the study site in 2021.

In the absence of any soil strength and unit weight data for study site, these parameter values were selected using the Quito Geotechnical Database, Quito/GEO-299 (Othman *et al.* 2022). This database comprises records of publicly available geotechnical testing results that have been collated, systematised, and statistically analysed to determine the most representative values for cangahua and other soils in the city (Hen-Jones *et al.* 2022, Othman *et al.* 2022). The CHASM input parameter dataset for the study site is presented in Table 1. To assess the influence of k_{sat} of slope stability we took a parametric modelling approach in which different values of k_{sat} were used in a series of CHASM simulations. To account for uncertainties in soil shear strength and rainfall intensity these input values were also varied. The selected parameter values are in the right-hand column of Table 1, giving total of 90 combinations and associated CHASM simulations. Each simulation runs for 360 hours with the rainfall imposed during hours 168-192.

3 SLOPE STABILITY SIMULATION RESULTS AND ANALYSIS

CHASM simulation outputs include the minimum value of F for each hour, the location of the associated slip surface, the failure mass, and the pore water pressures and moisture contents for each cell. In this study the minimum value of F for the whole simulation was taken as an indication of the overall sensitivity of slope stability to variations in k_{sat}, shear strength and rainfall (Table 2).

Table 2. CHASM simulations showing the effect of variations in k_{sat} at the study site, whilst also accounting for variations in shear strength and two rainfall intensities. Results show the minimum F with associated simulation hour in parenthesis. Rainfall is imposed during hours 168-192 and the simulation stops at hour 360. Dark shading, $F < 1$; light shading, $1 \geq F \geq 1.4$; no shading, $F > 1.4$.

		24-hour rainstorm, 5 mm/h (1.39×10^{-6} m/s)			24-hour rainstorm, 10 mm/h (2.78×10^{-6} m/s)		
		k_{sat} (m/s)			k_{sat} (m/s)		
ϕ' (°)	c' (kPa)	1×10^{-5}	1×10^{-6}	1×10^{-8}	1×10^{-5}	1×10^{-6}	1×10^{-8}
24	0 *	$0.64_{(193)}$	$0.6_{(before\ rain)}$	$0.88_{(before\ rain)}$	$0.51_{(before\ rain)}$	$0.6_{(before\ rain)}$	$0.88_{(before\ rain)}$
	5	$1.15_{(201)}$	$1.10_{(255)}$	$1.29_{(360)}$	$1.02_{(194)}$	$1.09_{(259)}$	$1.29_{(360)}$
	15	$1.76_{(195)}$	$1.74_{(285)}$	$1.79_{(360)}$	$1.75_{(218)}$	$1.74_{(285)}$	$1.79_{(360)}$
	30	$2.2_{(195)}$	$2.17_{(285)}$	$2.23_{(360)}$	$2.19_{(211)}$	$2.18_{(285)}$	$2.23_{(360)}$
	65	$3.22_{(195)}$	$3.20_{(285)}$	$3.26_{(360)}$	$3.21_{(211)}$	$3.2_{(285)}$	$3.26_{(360)}$
34	0 *	$0.81_{(before\ rain)}$	$0.78_{(before\ rain)}$	$1.27_{(before\ rain)}$	$0.68_{(before\ rain)}$	$0.77_{(before\ rain)}$	$1.27_{(before\ rain)}$
	5	$1.3_{(193)}$	$1.26_{(262)}$	$1.49_{(360)}$	$1.18_{(194)}$	$1.26_{(241)}$	$1.49_{(360)}$
	15	$2.39_{(201)}$	$2.39_{(265)}$	$2.45_{(360)}$	$2.3_{(193)}$	$2.38_{(268)}$	$2.45_{(360)}$
	30	$2.84_{(152)}$	$2.83_{(285)}$	$2.89_{(360)}$	$2.85_{(210)}$	$2.83_{(285)}$	$2.89_{(360)}$
	65	$3.65_{(273)}$	$3.7_{(354)}$	$3.86_{(360)}$	$3.63_{(354)}$	$3.7_{(339)}$	$3.86_{(360)}$
44	0 *	$1.03_{(before\ rain)}$	$1.00_{(before\ rain)}$	$1.05_{(before\ rain)}$	$0.91_{(before\ rain)}$	$0.99_{(before\ rain)}$	$1.05_{(before\ rain)}$
	5	$1.49_{(193)}$	$1.45_{(253)}$	$1.69_{(360)}$	$1.37_{(193)}$	$1.45_{(244)}$	$1.69_{(360)}$
	15	$2.69_{(202)}$	$2.65_{(257)}$	$2.83_{(360)}$	$2.56_{(193)}$	$2.64_{(278)}$	$2.83_{(360)}$
	30	$3.62_{(273)}$	$3.65_{(285)}$	$3.75_{(360)}$	$3.59_{(352)}$	$3.65_{(285)}$	$3.75_{(360)}$
	65	$3.87_{(218)}$	$3.92_{(355)}$	$4.09_{(360)}$	$3.83_{(352)}$	$3.92_{(339)}$	$4.09_{(360)}$

* For $c' = 0$ kPa this only applies to the top 1m of the colluvial cangahua to represent the possible effect of weathering in reducing cementation. In these scenarios the rest of the stratum was modelled with $c' = 5$ kPa.

The results in Table 2 show that c' is has the greatest influence on F. There is a direct relationship between an increase in these shear strength parameter values and an increase in F. Furthermore, analysis of hourly CHASM results within each simulation shows that for slopes where $c' = 5$kPa in the colluvial cangahua F drops sharply in response to rainfall and loss of matric suction at the critical slip

surface. For example, where $c' = 5$kPa, $\phi' = 24°$, $k_{sat} = 1\text{x}10^{-5}$ m/s and $I = 5$mm/h, F drops from 1.45 to 1.15 during the rainfall event and then recovers (Fig. 2a). Whereas, for simulations with higher values of c' and the same values of ϕ', k_{sat} and I, the values of F are constant throughout the simulations ($F = 1.76$, 2.2 and 3.22 for $c' = 15$kPa, 30kPa and 65kPa respectively), and are unaffected by rainfall.

The location of the critical slip circle is also affected by c'. For slopes where $c' = 0$kPa in the top 1m of colluvial cangahua (representing weathering) and 5kPa in the rest of that stratum, the slip circle is always in the top 1m with $F < 1$. Where $c' = 5$kPa throughout the colluvial cangahua, the slip circle is within the cut slope, and F typically drops below 1.4 after rainfall when $\phi' \leq 34°$. For all other slopes with higher shear strength, the critical slip circle is deeper within the colluvial cangahua and $F > 1.4$.

The influence of k_{sat} on F is most important for slopes with low c', in which k_{sat} determines the timing of the minimum value of F and the responsiveness of the slope stability to rainfall. As Fig. 2a shows, when slopes with $c' = 5$kPa have a high hydraulic conductivity ($k_{sat} = 1\text{x}10^{-5}$m/s) they show a significant decrease in F during the 24-hour rainfall event, which gradually recovers over the following 7 days. Where the same slope is modelled with medium hydraulic conductivity ($k_{sat} = 1\text{x}10^{-6}$ m/s) there is a similar behaviour except that once the rainfall is over, F does not recover as fast. In contrast, low hydraulic conductivity ($k_{sat} = 1\text{x}10^{-8}$ m/s) slopes show relatively constant stability over time. The reason for the slower and lower responsiveness of the medium and low k_{sat} slopes is that seepage is much slower within these slopes and pore water pressures are not varying as fast or as much as for the high k_{sat} slope. Furthermore, less rainfall will infiltrate into medium or low k_{sat} slopes.

The importance of k_{sat} for the stability of slopes with low c' is also seen when rainfall intensity is considered (Fig. 2b). For the most permeable slopes ($k_{sat} = 1\text{x}10^{-5}$m/s) with $c' = 5$kPa an increase in rainfall intensity from 5mm/h to 10mm/h results in a decrease in F due to a greater amount of water infiltrating the slope. However, for the $k_{sat} = 1\text{x}10^{-6}$ m/s and $k_{sat} = 1\text{x}10^{-8}$ m/s slopes the rainfall intensities of both storms exceed the hydraulic conductivity (i.e., exceeds the maximum rate at which the water can enter the slope). Any excess rainfall that cannot infiltrate into these medium and low k_{sat} slopes will be lost from the system – on a real slope it would translate into surface water runoff and in the numerical scheme of CHASM it is simply removed from the calculation.
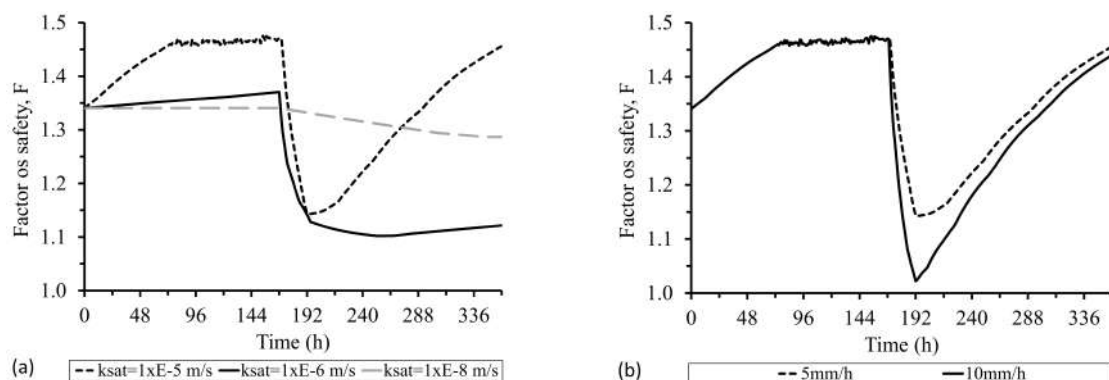
Figure 2. CHASM simulations of F over 360 hours (rainfall from hours 168 to 192): a) slopes with low shear strength ($c' = 5$kPa, $\phi' = 24°$), varying k_{sat} and a 5mm/h 24-hour rainfall event; b) slopes with high hydraulic conductivity ($k_{sat} = 1\text{x}10^{-5}$ m/s), exposed to two 24-hour storms of different intensities (5mm/h and 10mm/h)

4   DISCUSSION

Measurements of k_{sat} in the field are valuable for assessing slope stability in response to rainfall and changing groundwater conditions. Given the limited resources available for soil testing in cities such as Quito it is important for geotechnical engineers and city planners to know what priority to place on obtaining such data and how to interpret the results of any modelling studies in which it is used.

This study shows that for a typical colluvial cangahua slope in south Quito, c' has the largest effect on overall slope stability and the dynamic response to rainfall. For slopes with low shear strength properties, the influence of k_{sat} also becomes important. For example, for slopes modelled with $c' = 5$kPa and $\phi' \leq 34°$, higher values of k_{sat} result in $F < 1.4$ or, in some cases, close to $F = 1$ due to rainfall. Where c' of the top 1m of soil was modelled as 0kPa, such as might occur with weathering of the colluvial cangahua, CHASM indicated slope failure within this superficial layer before or during rainfall. This is in line of observations in the community of shallow slides during rainfall (and where CHASM indicated slope failure before rainfall, it was assumed that this combination of geotechnical property values would not exist in the field). Conversely, soils with $c' > 15$kPa exhibit $F > 1.4$ even when pore water pressures are increased by rainfall infiltration.

These results indicate that slopes with high k_{sat} and low shear strength properties are most responsive to rainfall and to possible increases in rainfall intensity due to climate change. For such slopes the minimum value of F decreases as rainfall intensity increases, up to the point where $I > k_{sat}$. The stability of slopes with low k_{sat} may be less affected by intense rainfall, but may generate more runoff, erosion and flash flooding. It may also be hypothesized that any potential increases in rainfall duration or an increasing frequency of rainfall events could still adversely affect the lower k_{sat} slopes by allowing infiltration over longer periods of time.

5 CONCLUSION

From the results of the CHASM simulations described in this paper, c' is shown to be the leading driver of slope instability. When this parameter has high values within the range established for the soils in Quito, it dominates the stability calculations regardless of the existence of variations in other parameters. However, for slopes with low values of c', simulations showed that k_{sat} also has an important influence on slope stability response to rainfall. This suggests that geotechnical engineers should continue efforts to characterise the shear strength properties of soils such as cangahua, and where c' is suspected to be low it is important to also estimate the k_{sat} of the soil mass in the field. The use of in-situ double-ring infiltrometers and community-based approaches to data acquisition could be helpful in data-scarce areas (e.g. Zapata *et al.* 2023). Future work should evaluate if there is a direct correlation between the degree of cementation of the cangahua soil type and the values of c' and k_{sat}.

REFERENCES

Almeida, S., Holcombe, E. A., Pianosi, F. and Wagener, T. (2017). Dealing with deep uncertainties in landslide modelling for disaster risk reduction under climate change. *Natural Hazards and Earth System Sciences* **17(2):** 225–241.

Anderson, M.G. (1990). *A Feasibility Study in Mathematical Modelling of Slope Hydrology and Stability.* Geotechnical Control Office, Civil Engineering Services Department, Hong Kong, Report CE 23/90.

Anderson M.G. and Howes S. (1985). Development and application of a combined soil water-slope stability model. *Quarterly Journal of Engineering Geology and Hydrogeology* **18(3):** 225–236.

Bishop, A.W. (1955). The use of the slip circle in the stability analysis of slopes. *Géotechnique*, **5(1):** 7–17.

Bozzolan, E., Holcombe, E., Pianosi, F. and Wagener, T. (2020). Including informal housing in slope stability analysis – an application to a data-scarce location in the humid tropics. *Natural Hazards and Earth System Sciences* **20(11):** 3161–3177.

Crespo, E. (1987). Slope stability of the Cangahua Formation, a volcaniclastic deposit from the Interandean Depression of Ecuador. *M.Sc. thesis*, Cornell University, Ithaca, NY.

Darcy, H. (1856). *Les Fontaines Publique de la Ville de Dijon*. Dalmont, Paris, France (in French).

Emberson, R., Kirschbaum, D. and Stanley, T. (2020). New global characterisation of landslide exposure. *Natural Hazards and Earth System Sciences* **20(12):** 3413–3424.

Feng, S. (2022). Hydraulic Conductivity of Road Construction Materials: with a focus on freeze-thaw effects. *Ph.D. thesis*, University of Bristol, Bristol, UK.

Hen-Jones, R., Vardanega, P.J., Zapata, C., Jiménez, E. and Holcombe, E.A. (2022). Developing a geotechnical database to improve slope stability assessments in Quito, Ecuador. In: Rahman, M.M. and Jaksa, M. (eds.) *Proceedings of Twentieth International Conference on Soil Mechanics and Geotechnical Engineering (ICSMGE 2022)*, Australian Geomechanics Society, Sydney, Australia, **2:** 2569-2574.

Hodnett, M.G. and Tomasella, J. (2002). Marked differences between van Genuchten soil water-retention parameters for temperate and tropical soils: a new water-retention pedo-transfer functions developed for tropical soils. *Geoderma*, **108(3-4):** 155–180.

Holcombe, E.A., Beesley, M.E.W., Vardanega, P.J. and Sorbie, R. (2016). Urbanisation and landslides: hazard drivers and better practices. *Proceedings of the Institution of Civil Engineers - Civil Engineering* **169(3):** 137–144.

Hubble, T.C.T., Airey, D.W., Sealy, H.K., De Carli, E.V. and Clarke, S.L. (2013). A little cohesion goes a long way: estimating appropriate values of additional root cohesion for evaluating slope stability in the Eastern Australian Highlands. *Ecological Engineering* **61(C):** 621–632.

Municipio de Quito (2022). La Gasca and La Comuna: 6 months after the flood. Press Release. Available at: http://www.quitoinforma.gob.ec/2022/08/01/la-gasca-y-la-comuna-seis-meses-despues-del-aluvion/ [03/04/2023].

O'Rourke, T.D. and Crespo, E. (1988). Geotechnical properties of cemented volcanic soil. *Journal of Geotechnical Engineering (ASCE)* **114(10):** 1126–1147.

Othman, M., Hen-Jones, R., Zapata, C., Jiménez, E., De Luca, F., Holcombe, E.A. and Vardanega, P.J. (2022). Quito Geotechnical Database (Quito/GEO-299 v.1.0). University of Bristol, Bristol, UK. https://doi.org/10.5523/bris.3m2ficmw3ltjx2m0yl4cwptkqm

Ozturk, U., Bozzolan, E., Holcombe, E.A., Shukla, R., Pianosi, F. and Wagener, T. (2022). How climate change and unplanned urban sprawl bring more landslides. *Nature* **608:** 262-265.

Picarelli, L., Lacasse, S. and Ho, K.K.S. (2021). The impact of Climate Change on landslide Hazard and Risk. In: Sassa, K. *et al.* (eds) *Understanding and Reducing Landslide Disaster Risk. WLF 2020. ICL Contribution to Landslide Disaster Risk Reduction*. Springer, Cham, 131-141.

Richards, L.A. (1931). Capillary conduction of liquids in porous mediums. *Journal of Applied Physics* **1(5):** 318–333.

Shepheard, C.J., Vardanega, P.J., Holcombe, E.A. and Michaelides, K. (2018). Analysis of design choices for a slope stability scenario in the humid tropics. *Proceedings of the Institution of Civil Engineers - Engineering Sustainability* **171(1):** 37–52.

UNDRR (2022). Global Assessment Report on Disaster Risk Reduction 2022: *Our World at Risk: Transforming Governance for a Resilient Future*. United Nations Office for Disaster Risk Reduction: Geneva.

UN Populations Division (2018). World Urbanization Prospects 2018. United Nations Population Division. Available at: https://population.un.org/wup/Publications/Files/WUP2018-Report.pdf [03/04/2023].

Vera, R. and Lopez, R. (1992). Tipologia de la cangahua. In: Zebrowski, C. *et al.* (eds.), *Terra, Numero Especial Suelos Volcánicos Endurecidos* **10:** 113-119 (In Spanish).

Watson, C.S., Elliott, J.R., Ebmeier, S.K., Vásquez, M.A., Zapata, C., Bonilla-Bedoya, S., Cubillo, P., Orbe, D. F., Córdova, M., Menoscal, J. and Sevilla, E. (2022) Enhancing disaster risk resilience using greenspace in urbanising Quito, Ecuador, *Natural Hazards and Earth System Sciences* **22(5):** 1699–1721.

Wilkinson. P.L., Anderson, M.G. and Lloyd, D.M. 2002. An integrated hydrological model for rain-induced landslide prediction. *Earth Surface Processes and Landforms* **27(12):** 1285–1297.

Wu, T.H., McKinnell III, W.P. and Swanston, D.N. (1979). Strength of tree roots and landslides on Prince of Wales Island, Alaska. *Canadian Geotechnical Journal* **16(1):** 19–33.

Zapata, C., Feng, S., Holcombe, E.A., Vardanega, P.J. and Jiménez, E. (2023). Measurement of field hydraulic conductivity for a Quito soil. *17th Asian Regional Conference on Soil Mechanics and Geotechnical Engineering*, accepted for publication.